Journal of the Korean Ceramic Society
Vol. 54, No. 4, pp. 303~307, 2017.

https://doi.org/10.4191/kcers.2017.54.4.01

Highly Sensitive and Selective Ethanol Sensors Using Magnesium doped Indium Oxide Hollow Spheres

Young-Moo Jo*, Chul-Soon Lee*, Rui Wang*, Joon-Shik Park, and Jong-Heun Lee*,†**

**Department of Materials Science and Engineering, Korea University, Seoul 02841, Korea*
***Smart Sensor Research Center, Korea Electronic Technology Institute, Seongnam 13509, Korea*

(Received May 13, 2017; Revised June 4, 2017; Accepted June 5, 2017)

ABSTRACT

Pure In_2O_3, 0.5 and 1.0 wt% Mg doped In_2O_3 hollow spheres were synthesized by ultrasonic spray pyrolysis of a solution containing In-, Mg-nitrate and sucrose and their gas sensing characteristics to 5 ppm C_2H_5OH, *p*-xylene, toluene, and HCHO were measured at 250, 300 and 350°C. Although the addition of Mg decreases the specific surface area and the volume of meso-pores, the gas response (resistance ratio) of the 0.5 wt% Mg doped In_2O_3 hollow spheres to 5 ppm C_2H_5OH at 350°C (69.4) was significantly higher than that of the pure In_2O_3 hollow spheres (24.4). In addition, the Mg doped In_2O_3 hollow spheres showed the highest selectivity to C_2H_5OH. This was attributed to the dehydrogenation of C_2H_5OH assisted by basic MgO into reactive CH_3CHO and H_2.

Key words : Sensors, Electrical properties, Gas sensor, Indium oxide, Magnesium

1. Introduction

Gas sensors are used extensively in many fields, including industrial safety, environment, and life and health applications. Oxide semiconductor-type gas sensors exhibit chemiresistive variation by the reaction between analyte gas and the oxygen molecules adsorbed to the sensing material surface. Main advantages of oxide semiconductor-type gas sensors are simple working principle, high sensitivity, facile miniaturization, and rapid gas response.[1)]

Most gas sensing materials that have been studied to date are n-type oxide semiconductors, including SnO_2,[2,3)] ZnO,[4,5)] TiO_2,[6)] and In_2O_3.[7)] Among these, In_2O_3 has drawn attention as a material suitable for wearable and flexible devices because of its transparency and high conductivity.[8)] In addition, many studies have been conducted using In_2O_3 nanoparticles in gas sensors, have a high sensitivity to reducing gases. The resistance of n-type oxide semiconductors is increased when oxygen is adsorbed to the surface of the particle, which is then negatively charged, because an electron depletion layer is formed near the particle surface. If reducing gases, such as C_2H_5OH, *p*-xylene, toluene, and HCHO, react with the oxygen adsorbed with negative charge, the electrons are transported to the inside of the n-type oxide semiconductors, resulting in a decrease in resistance, due to the thinning of the electron depletion layer.[9)] Liang *et al.* improved the hydrogen sulfide sensing characteristics of a sensor by using indium oxide containing a copper oxide as the gas sensing substance,[10)] and Rai *et al.* significantly increased gas sensing characteristics by employing a Pd-doped indium oxide.[11)]

Oxide-based nanostructures which have a large specific surface area, such as hollow structures,[12)] nanowires,[4,13)] nanofibers,[3,5,10)] hierarchical structures,[14)] and porous nanostructures,[15)] can also improve gas sensitivity, and have been extensively applied to gas sensors. The methods for synthesizing oxide nanostructures include the hydrothermal method,[7,14)] electrospinning,[3,5,10)] and ultrasonic spray pyrolysis.[12,15,16,17)] In ultrasonic spray pyrolysis, microdroplets generated by ultrasonic transduction are thermally pyrolyzed in a high-temperature electric furnace to synthesize porous hollow nanostructures. This method is easy and simple, and enables mass production and facile control of composition and doping.[17)]

In the present study, pure and Mg-doped In_2O_3 spheres were prepared using ultrasonic spray pyrolysis to investigate the effect of Mg doping on the gas sensing characteristics of In_2O_3 spheres. The result showed that Mg doping at specific concentrations significantly enhanced the response and selectivity for ethanol. The gas sensing mechanism was also investigated in relation to Mg additive.

2. Experimental Procedure

2.1. Synthesis of In_2O_3

A spray solution for the synthesis of In_2O_3 hollow nanoparticles was prepared using the following procedures. 7.52 g of $In(NO_3)_3 \cdot xH_2O$ (99.99%, Sigma-Aldrich Co., Ltd., USA) and 17.11 g of sucrose (99.5%, Sigma-Aldrich Co., Ltd., USA) were added to 500 ml of distilled water. The resulting

†Corresponding author : Jong-Heun Lee
E-mail : jongheun@korea.ac.kr
Tel : +82-2-3290-3282 Fax : +82-2-928-3584

mixture solution was stirred for 2 h. Spray solutions for the synthesis of In_2O_3 hollow nanoparticles doped with 0.5 wt% and 1.0 wt% Mg were also prepared by the same method. 0.15 and 0.29 g $Mg(NO_3)_2 \cdot 6H_2O$ (99.99%, Sigma-Aldrich Co., Ltd., USA) and 7.34 and 7.18 g $In(NO_3)_3 \cdot xH_2O$ were respectively added to 500 ml of distilled solution with 17.11 g of sucrose, and the resulting solutions were stirred. The molar concentrations of the metal ions and sucrose were fixed at 0.05 M and 0.1 M, respectively.

The mixed solutions were sprayed as small droplets by applying ultrasound (with a resonance frequency of 1.7 MHz), and the sprayed droplets were transported by a carrier gas (O_2, 10 L/min) to an electric furnace at 900°C where the droplets underwent pyrolysis. Synthesized precursor spherical particles were collected by using a bag filter and then thermally treated to obtain pure In_2O_3 and 0.5 wt% and 1 wt% Mg-doped In_2O_3 hollow nanoparticles (referred to as In_2O_3, 0.5Mg-In_2O_3, and 1.0Mg-In_2O_3, respectively).

2.2. Sample Analysis

A field emission-scanning electron microscope (FE-SEM, S-4300, Hitachi) and a transmission electron microscope (TEM, Talos F200X, FEI) were used to analyze the shapes of the synthesized powders. An X-ray diffractometer (Rigaku D/MAX-2500V/PC, CuKα line = 1.5418 Å) was used to analyze the crystal structure of the substances. Brunauer-Emmett-Teller method (BET, Tristar 3000, Micrometrics) was employed to verify the specific area and pore distribution of the particles.

2.3. Fabrication and Measurement of Sensor Device

The synthesized hollow nanoparticles were mixed with distilled water as a slurry, which was coated on an alumina substrate with two Au electrodes to fabricate a gas sensor device. The water residue in the coated sensor substance was eliminated and the sensor device was stabilized by performing thermal treatment at 500°C for 3 h, using a heater formed at the backside of the substrate. Then, the gas responses were measured. The gas flow rate was fixed at 200 cm^3/min. The response was measured with four reducing gases, C_2H_5OH, *p*-xylene, toluene, and HCHO, at a concentration of 5 ppm at temperatures of 250, 300, and 350°C.

3. Results and Discussion

3.1. Shape and Phase of Synthesized Powder

The structures synthesized by ultrasonic spray pyrolysis were spherical regardless of the composition. The diameter of the spherical particles ranged from 500 nm to 1 μm, showing a relatively uniform size distribution (Figs. 1(a) to 1(f)). In the TEM images, the centers of the spherical 0.5Mg-In_2O_3 and 1.0Mg-In_2O_3 particles were found to be bright, indicating that the particles had a hollow structure (Figs. 2(a), 2(b), 2(f), and 2(g)). The thickness of the hollow structure shell layer was found to be about 16 nm (Figs. 2(b) and 2(g)). The spherical indium salt-carbon composites were synthesized at the beginning stage of spray pyrolysis, and the hollow structure may have been formed when the carbon component was removed during the later stage of pyrolysis reaction. The energy dispersive spectrometer (EDS) analysis showed that the Mg components was uniformly doped in all the regions of the In_2O_3 particles, rather than being aggregated with each other (Figs. 2(c) to 2(e) and 2(h) to 2(j)).

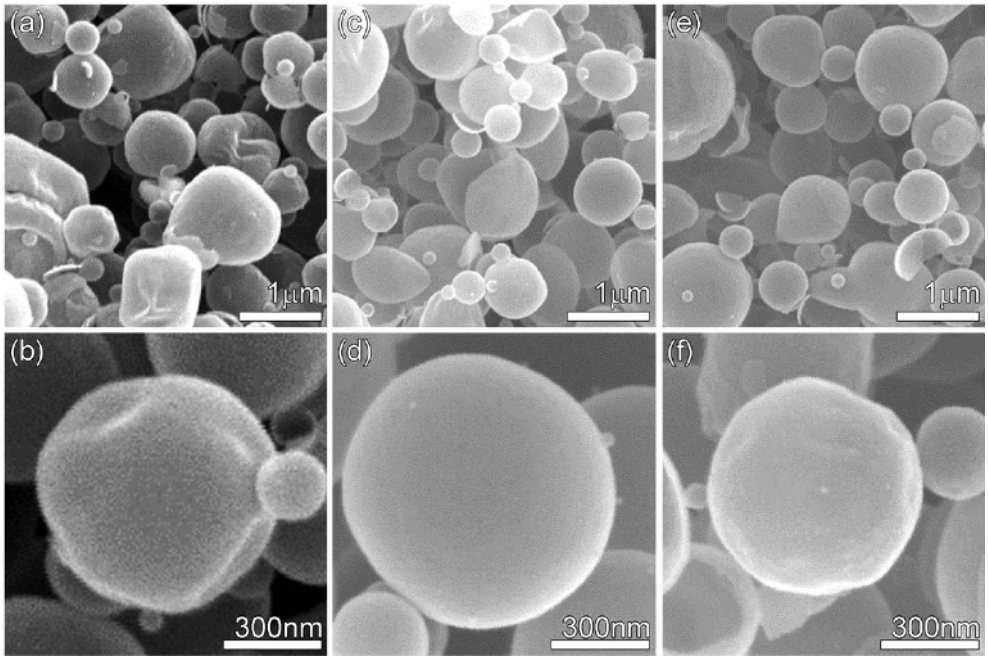

Fig. 1. SEM images of (a-b) pure-In_2O_3, (c-d) 0.5Mg-In_2O_3 and (e-f) 1.0Mg-In_2O_3 spheres prepared by spray pyrolysis reaction and subsequent heat treatment at 600°C for 3 h.

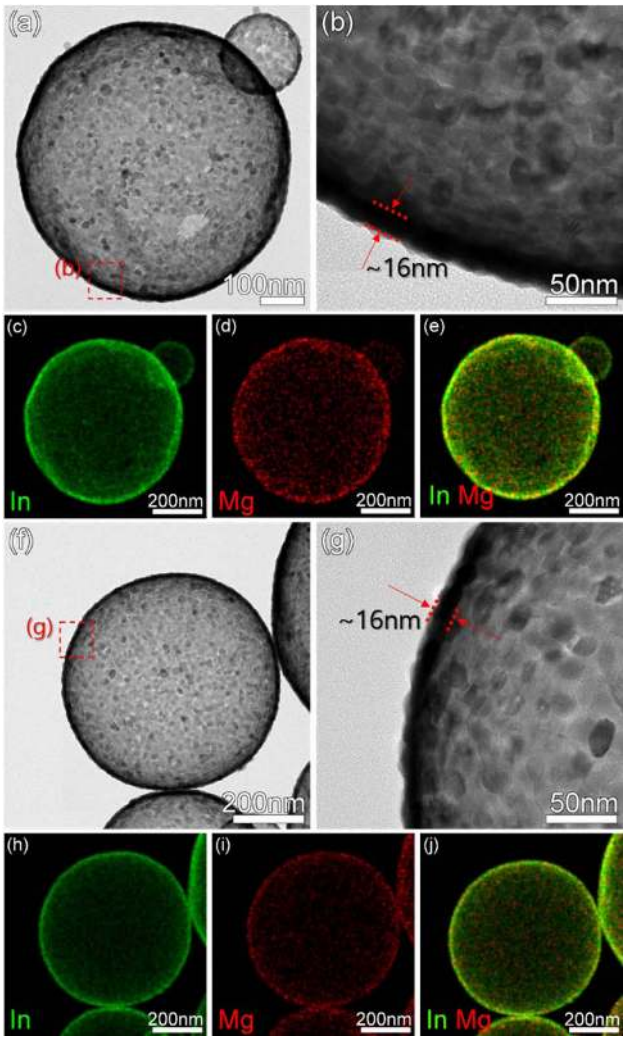

Fig. 2. TEM images and elemental mapping of (a-e) 0.5Mg-In_2O_3 and (f-j) 1.0Mg-In_2O_3 powders.

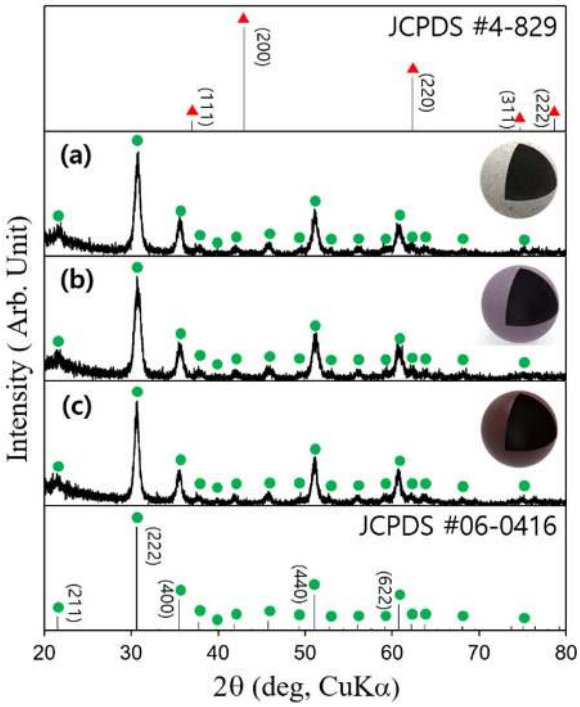

Fig. 3. X-ray diffraction patterns (XRD) of (a) pure-, (b) 0.5Mg-In_2O_3 and (c) 1.0Mg-In_2O_3 powders.

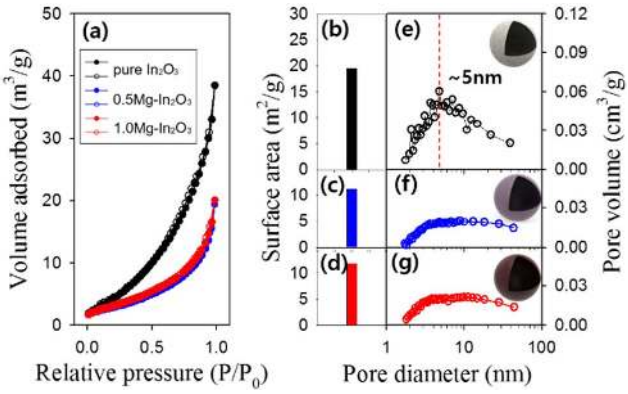

Fig. 4. (a) N_2 adsorption/desorption isotherms of In_2O_3 (black), 0.5Mg-In_2O_3 (blue) and 1.0Mg-In_2O_3 (red). (b-g) Corresponding BET surface areas and pore-size distribution of (b, e) In_2O_3, (c, f) 0.5Mg-In_2O_3 and (d, f) 1.0Mg-In_2O_3 powders.

The X-ray diffraction analysis of the synthesized power showed In_2O_3 to have a body centered cubic structure (JCPDS #06-0416), but no Mg oxide-related phase was found (JCPDS #4-829) (Fig. 3). At the coordination number (CN) of 6, the ionic radius of Mg^{2+} is 0.86 Å, which is slightly smaller than that of In^{3+} (0.94 Å) with the same CN. The X-ray diffraction result suggests that Mg is doped into the In_2O_3 lattice,[18] or a small quantity of Mg-related secondary phase may have not been detected due to the detection limit of the X-ray diffractometer. The calculation based on the Scherrer's equation revealed that the primary particle diameter of the In_2O_3, 0.5Mg-In_2O_3, and 1.0Mg-In_2O_3 powders were 12.4, 11.4, and 13.5 nm, respectively.

3.2. Specific Surface Area and Pore Distribution

The pore size and volume were measured by BET analysis (Fig. 4). The specific surface area of the 0.5Mg-In_2O_3 and 1.0Mg-In_2O_3 microparticles were 11.1 m^3/g and 11.9 m^3/g, respectively, which is about half of the specific surface area of pure-In_2O_3 (19.5 m^3/g) (Figs. 4(a) to 4(d)). The mesopores, with diameters of about 5 nm, was decreased by the Mg doping (Figs. 4(e) to 4(g)), indicating that the specific surface area was decreased because the inserted Mg components blocked the pores.

3.3. Evaluation of Gas Response

The gas sensing characteristics were measured after stabilizing the sensing substances through thermal treatment for more than 1 h at 250, 300, and 350°C. The gases undergoing the sensing test were C_2H_5OH, xylene, toluene, and HCHO at 5 ppm. The gas response was defined as R_a/R_g

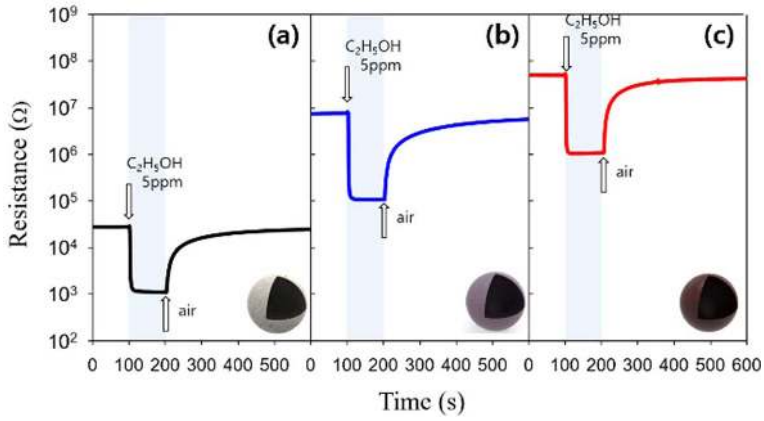

Fig. 5. Gas sensing transients of (a) In_2O_3, (b) 0.5Mg-In_2O_3 and (c) 1.0Mg-In_2O_3 hollow spheres to 5 ppm C_2H_5OH at 350°C.

where R_a denotes the resistance in the air and R_g the resistance in the gas.

The responses to 5 ppm C_2H_5OH measured at 350°C with In_2O_3, 0.5Mg-In_2O_3, and 1.0Mg-In_2O_3 were 24.4, 69.4, and 46.3, respectively (Figs. 5 and 6). This verified that the doping of Mg effectively increased the response of the In_2O_3 sensor. The sensor resistance in the air (R_a) was increased from 27.3 KΩ (In_2O_3) by 270 times and 1,840 times to 7.5 MΩ and 50.3 MΩ in the 0.5Mg-In_2O_3 and 1.0Mg-In_2O_3, respectively, depending on the quantity of doped Mg. This indicated that the doping of Mg^{2+} played the role of an electron accepter to increase the overall resistance (Fig. 5). Assuming that a certain number of electrons are injected to the sensor through the gas sensing reaction, the response of Mg-doped In_2O_3 will be higher because the electron concentration in the sensor is significantly lower. This may be a possible explanation of the increase of the gas response by Mg doping.

The gas response of individual powders was measured at all temperatures with all the test gases. The results showed that the response was highest for the C_2H_5OH sensing with the pure In_2O_3 sensor, and the Mg-doped In_2O_3 sensors (Fig. 6). Generally, the response of the n-type oxide semiconductor gas sensors to *p*-xylene, toluene and HCHO was lower than that of C_2H_5OH, because the gas reactivity with C_2H_5OH was highest, which is consistent with the result of the present study.

In comparison with pure In_2O_3, the addition of Mg greatly increased the response to C_2H_5OH but slightly increased or even decreased the response to *p*-xylene, toluene, and HCHO, which are representative indoor hazardous gases. The selectivity to C_2H_5OH was calculated by dividing the response to C_2H_5OH with the response of other gases ($S_{C2H5OH}/S_{analyte\ gas}$) (Fig. 7). The $S_{C2H5OH}/S_{analyte\ gas}$ value of the Mg-doped In_2O_3 sensors was significantly higher than that of the pure In_2O_3 sensor, indicating that the addition of Mg increased not only the response to C_2H_5OH but also the selectivity to C_2H_5OH.

The increase in the response and the selectivity may be explained by the difference in reactivity between the C_2H_5OH and the acid-base surface. It has been reported that a dehy-

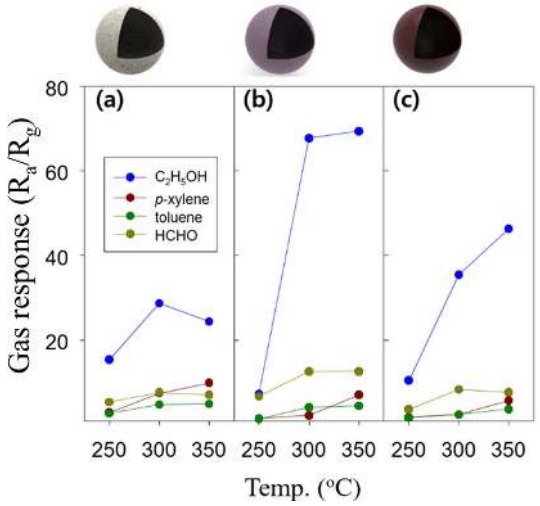

Fig. 6. Responses of (a) In_2O_3, (b) 0.5Mg-In_2O_3 and (c) 1.0Mg-In_2O_3 hollow spheres to 5 ppm of analyte gases at 250, 300 and 350°C (5 ppm C_2H_5OH, *p*-xylene, toluene, HCHO).

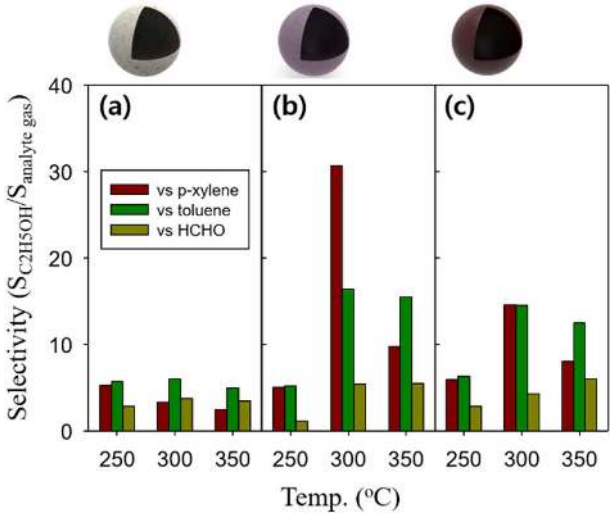

Fig. 7. C_2H_5OH selectivity ($S_{C2H5OH}/S_{analyte\_gas}$) of (a) In_2O_3, (b) 0.5Mg-In_2O_3 and (c) 1.0Mg-In_2O_3 hollow spheres to 5 ppm of analyte gases at 250, 300 and 350°C.[17]

drating reaction occurs between C_2H_5OH and an acidic surface to result in the decomposition to C_2H_4 (g) and H_2O (g), while a dehydrogenation reaction occurs between C_2H_5OH and a basic surface to result in the decomposition to CH_3CHO (g) and H_2 (g).[13,19] The CH_3CHO (g) and H_2 (g) generated from the basic surface react with the negatively charged oxygen on the oxide surface better than the C_2H_4 (g) and H_2O (g) generated from the acidic surface, donating more electrons and showing a higher gas response. Since Mg is a representative alkaline substance, the C_2H_5OH dehydrogenation reaction enhanced by the Mg doping might have increased the response and selectivity to C_2H_5OH.

4. Conclusions

Hollow spherical particles of pure-In_2O_3 and 0.5 wt% and 1.0 wt% Mg-doped In_2O_3 were synthesized by ultrasonic spray pyrolysis, and their gas response was evaluated. The C_2H_5OH gas response was greatly improved by the addition of Mg. Particularly in the sensor to which 0.5 wt% Mg was added, the highest ethanol response was found at 350°C, and the highest *p*-xylene selectivity was found at 300°C. The C_2H_5OH gas response and selectivity were increased because alkaline Mg decomposed the C_2H_5OH into CH_3CHO and H_2, increasing the gas response, and because the addition of Mg decreased the background electron concentration of the sensor in air, making the resistance more sensitive to the gaseous reaction. The results of the present study show that Mg-doped oxides may be used to sense C_2H_5OH gas with high response and high selectivity.

Acknowledgements

This work is supported by the "S/W Converged Components Technology Development Program" (project No. 10043800) by KEIT and MOTIE in the Korea and Brain Pool Program (No. 161S-2-3-1544), through the Korean Federation of Science and Technology Societies (KOFST), funded by the Ministry of Science, ICT and Future Planning.

REFERENCES

1. N. Yamazoe, "Toward Innovations of Gas Sensor Technology," *Sens. Actuator, B,* **108** [1] 2-14 (2005).
2. B.-Y. Kim, J. S. Cho, J.-W. Yoon, C. W. Na, C.-S. Lee, J. H. Ahn, Y. C. Kang, and J.-H. Lee, "Extremely Sensitive Ethanol Sensor Using Pt-doped SnO_2 Hollow Nanospheres Prepared by Kirkendall Diffusion," *Sens. Actuator, B,* **234** 353-60 (2016).
3. J. W. Jung, S. J. Park, I. B. Jeong, B.-Y. Kim, and J.-H. Lee, "Design of Highly Reliable Thick Film Gas Sensor Using SnO_2 Nanofibers," *J. Sensor Sci. & Tech.*, **25** [4] 271-74 (2016).
4. H.-S. Woo, C.-H. Kwak, J.-H. Chung, and J.-H. Lee, "Highly Selective and Sensitive Xylene Sensors Using Ni-doped Branched ZnO Nanowire Networks," *Sens. Actuator, B,* **216** 358-66 (2015).
5. B.-Y. Kim, J.-W. Yoon, C.-S. Lee, J.-S. Park, and J.-H. Lee, "Trimethylamine Sensing Characteristics of Molybdenum doped ZnO Hollow Nanofibers Prepared by Electrospinning," *J. Sensor Sci. & Tech.*, **24** [6] 419-22 (2015).
6. A. M. Ruiz, G. Sakai, A. Cornet, K. Shimanoe, and J. R. Morante, "Cr-doped TiO_2 Gas Sensor for Exhaust NO_2 Monitoring," *Sens. Actuator, B,* **93** [1] 509-18 (2003).
7. K.-I. Choi, H.-R. Kim, and J.-H. Lee, "Enhanced CO Sensing Characteristics of Hierarchical and Hollow In_2O_3 Microspheres," *Sens. Actuator, B,* **138** [2] 497-503 (2009).
8. J.-C. Park, S.-J. Kang, and Y.-S. Yoon, "Properties of IZTO Thin Films Deposited on PEN Substrates with Different Working Pressures," *J. Korean Ceram. Soc.*, **52** [3] 224-27 (2015).
9. N. Yamazoe, G. Sakai, and K. Shimanoe, "Oxide Semiconductor Gas Sensors," *Catal. Surv. Asia*, **7** [1] 63-75 (2003).
10. X. Liang, T.-H. Kim, J.-W. Yoon, C.-H. Kwak, and J.-H. Lee, "Ultrasensitive and Ultraselective Detection of H_2S Using Electrospun CuO-loaded In_2O_3 Nanofiber Sensors Assisted by Pulse Heating," *Sens. Actuator, B,* **209** 934-42 (2015).
11. P. Rai, J.-W. Yoon, C.-H. Kwak, and J.-H. Lee, "Role of Pd Nanoparticles on Gas Sensing Behaviour of Pd@In_2O_3 Yolk-Shell Nanoreactors," *J. Mater. Chem. A*, **4** [1] 264-69 (2016).
12. Y. H. Cho, X. Liang, Y. C. Kang, and J.-H. Lee, "Ultrasensitive Detection of Trimethylamine Using Rh-doped SnO_2 Hollow Spheres Prepared by Ultrasonic Spray Pyrolysis," *Sens. Actuator, B,* **207** 330-37 (2015).
13. C.-H. Kwak, H.-S. Woo, F. Abdel-Hady, A. A. Wazzan, and J.-H. Lee, "Vapor-Phase Growth of Urchin-like Mg-doped ZnO Nanowire Networks and their Application to Highly Sensitive and Selective Detection of Ethanol," *Sens. Actuator, B,* **223** 527-34 (2016).
14. H.-J. Kim, J.-W. Yoon, K.-I. Choi, H. W. Jang, A. Umar, and J.-H. Lee, "Ultraselective and Sensitive Detection of Xylene and Toluene for Monitoring Indoor Air Pollution Using Cr-doped NiO Hierarchical Nanostructures," *Nanoscale,* **5** [15] 7066-73 (2013).
15. J.-W. Yoon, S. H. Choi, J.-S. Kim, H. W. Jang, Y. C. Kang, and J.-H. Lee, "Trimodally Porous SnO_2 Nanospheres with Three-Dimensional Interconnec-tivity and Size Tunability: A One-Pot Synthetic Route and Potential Application as an Extremely Sensitive Ethanol Detector," *NPG Asia Mater.*, **8** e244 (2016).
16. T.-H. Kim, J.-W. Yoon, and J.-H. Lee, "A Volatile Organic Compound Sensor Using Porous Co_3O_4 Spheres," *J. Korean Ceram. Soc.*, **53** [2] 134-38 (2016).
17. G. L. Messing, S.-C. Zhang, and G. V. Jayanthi, "Ceramic Powder Synthesis by Spray Pyrolysis," *J. Am. Ceram. Soc.*, **76** [11] 2707-26 (1993).
18. R. D. Shannon, "Revised Effective Ionic Radii and Systematic Studies of Interatomic Distances in Halides and Chalcogenides," *Acta Cryst.*, **A32** [5] 751-67 (1976).
19. T. Jinkawa, G. Sakai, J. Tamaki, N. Miura, and N. Yamazoe, "Relationship between Ethanol Gas Sensitivity and Surface Catalytic Property of Tin Oxide Sensors Modified with Acidic or Basic Oxides," *J. Mol. Catal. A: Chem.*, **155** 193-200 (2000).